
Article:
Curley, P., Giardiello, M. orcid.org/0000-0003-0560-4711, Liptrott, N.J. et al. (8 more authors) (2017) In vitro characterisation of solid drug nanoparticle compositions of efavirenz in a brain endothelium cell line. Journal of Interdisciplinary Nanomedicine, 2 (3). pp. 157-169. ISSN 2058-3273

https://doi.org/10.1002/jin2.32

Journal of Interdisciplinary Nanomedicine

BRITISH SOCIETY FOR NANOMEDICINE

Open Access

Journal of Interdisciplinary Nanomedicine ISSN 2058-3273

ORIGINAL ARTICLE

In vitro characterisation of solid drug nanoparticle compositions of efavirenz in a brain endothelium cell line

Paul Curley,[1] Marco Giardiello,[2] Neill J. Liptrott,[1,3] David Dickens,[1] Darren M. Moss,[1] James J. Hobson,[2] Alison C. Savage,[2] Tom O. McDonald,[2] Marco Siccardi,[1] Steve Rannard[2,3*] & Andrew Owen[1,3**]

[1] *Molecular and Clinical Pharmacology, Institute of Translational Medicine, University of Liverpool, Liverpool, UK*

[2] *Department of Chemistry, University of Liverpool, Crown Street, Liverpool, UK*

[3] *European Nanomedicine Characterisation Laboratory, Molecular and Clinical Pharmacology, Institute of Translational Medicine, University of Liverpool, Liverpool, UK*

Keywords
Blood brain barrier, Central nervous system, Efavirenz, Endocytosis, Solid drug nanoparticle.

Correspondence
Andrew Owen, Molecular and Clinical Pharmacology, Institute of Translational Medicine, University of Liverpool, UK.
Tel: +44 (0) 151 794 8211;
Fax: + 44 (0) 151 794 5656;
E-mail: aowen@liverpool.ac.uk
Steve Rannard, Department of Chemistry, University of Liverpool, UK.
Tel: +44 (0) 151 794 3501;
E-mail: srannard@liverpool.ac.uk

Received: 26 April 2016;
Revised: 30 June 2017;
Accepted: 10 August 2017

Journal of Interdisciplinary Nanomedicine, 2017; 2(3), doi: 10.1002/jin2.32

Abstract

The antiretroviral drug efavirenz displays many desirable pharmacokinetic properties such as a long half-life enabling once daily dosing but suffers from central nervous system safety issues. Various nanotechnologies have been explored to mitigate some of the limitations with efavirenz. While there has been progress in increasing the bioavailability, there has been no attempt to assess the impact of increased exposure to efavirenz on central nervous system safety. The uptake of aqueous and solid drug nanoparticle (SDN) formulations of efavirenz was assessed in the human cerebral microvessel endothelial cells/D3 brain endothelial cell line. The mechanisms of uptake were probed using a panel of transport and endocytosis inhibitors. The cellular accumulation of an efavirenz aqueous solution was significantly reduced by amantadine, but this was not observed with SDNs. The uptake of efavirenz SDNs was reduced by dynasore, but concentrations of the efavirenz aqueous solution were not affected. These data indicate that efavirenz is a substrate for transporters in brain endothelial cells (amantadine is an inhibitor of organic cation transporters 1 and 2), and formation of SDNs may bypass this interaction in favour of a mechanism involving dynamin-mediated endocytosis.

Introduction

The non-nucleoside reverse transcriptase inhibitor efavirenz (EFV) has been used in first-line human immunodeficiency virus therapy for over 15 years (Raffi et al., 2014). Efavirenz displays potent activity against wild-type human immunodeficiency virus-1, with an

IC_{50} of 0.51 ng/mL, inhibition constant (K_i) 2.93 nmol/L and a long plasma half-life of 40–76 h, enabling once daily dosing (Adkins and Noble, 1998; Best et al., 2011). Despite these favourable properties, EFV has very poor water solubility (<10 μg/mL) and bioavailability can be poor resulting in highly variable plasma exposure after oral administration (Siccardi et al., 2015).

Recently, we reported an EFV solid drug nanoparticle (SDN) formulation manufactured using an emulsion-templated freeze-drying (ETFD) approach (McDonald et al., 2014). Solid drug nanoparticles containing 70 wt% drug relative to polymer and surfactant excipients were successfully generated and displayed augmented transcellular permeation across Caco-2 cells with reduced cytotoxicity. Moreover, in vivo pharmacokinetic studies performed in rats demonstrated an increase in plasma EFV concentrations of approximately fourfold following a single oral dose (McDonald et al., 2014). Using SDNs, manufactured using ETFD, but composed of fluorescence resonance energy transfer dyes, intact particles were demonstrated to traverse an intact Caco-2 monolayer (McDonald et al., 2012).

If intact SDNs enter the systemic circulation after oral administration, a differential passage across the blood brain barrier (BBB) may be predicted. Importantly, this may influence EFV-associated neurocognitive adverse events such as depression, anxiety, and abnormal dreams (Sanchez Martin et al., 2013), which are known to negatively impact treatment (Leutscher et al., 2013).

One of the major obstacles to drug permeation into the brain is the battery of transport proteins within the brain endothelium (Al-Ghananeem et al., 2013; Yilmaz et al., 2012). Many antiretrovirals are substrates for one or more drug transporters, which limit or completely extrude them from the brain (Ene et al., 2011); however, the interaction of EFV with transporters has not been thoroughly characterised.

Although there have been genetic associations between *ABCB1* polymorphisms with EFV pharmacodynamics (Fellay et al., 2002), in vitro evidence indicates that EFV is not a substrate for P-gp (Janneh et al., 2009; Leschziner et al., 2007). Some evidence indicates that EFV may be a substrate for Breast Cancer Resistance Protein (BCRP) (ATP-binding cassette subfamily G member 2 (ABCG2)) and an ex vivo model showed increased mucosal to serosal permeation of EFV in everted gut sacs (Peroni et al., 2011). Efavirenz may also be a substrate for one or more solute carrier organic anion transporters, because its cellular accumulation was reduced by montelukast and estrone-3-sulphate (Janneh et al., 2009). However, convincing data regarding substrate affinity of EFV for active transport systems have remained elusive.

Although the size of a nanoparticle may preclude interactions with transport proteins, other methods of cellular uptake may affect them. Endocytosis includes multiple mechanisms such as clathrin-mediated endocytosis, calveolae-mediated endocytosis, and micropinocytosis that mammalian cells have developed for the uptake of molecules from the extracellular environment (Mukherjee et al., 1997). Macropinocytosis is typically involved in uptake of larger particles (<2 μM), whereas clathrin-mediated (<300 nm) and caveolae-mediated (<80 nm) endocytosis may predominate for smaller particles (Canton and Battaglia, 2012).

This study investigated differential uptake of EFV SDNs relative to an aqueous solution in the human cerebral microvessel endothelial cells (hCMEC)/D3 cell line in vitro, which is derived from human microvascular brain endothelial cells (Alfirevic et al., 2015; Dickens et al., 2012; Weksler et al., 2013). The hCMEC/D3 was selected for its frequent application as an in vitro model and characterisation as an immortalised BBB cell line. The HCMEC/D3 cell line exhibits many of the characteristics of the BBB, such as expression of protein necessary for tight junction formation, polarised expression of multiple transporter proteins (including P-gp, BCRP, and organic cation transporters) (Poller et al., 2008; Sekhar et al., 2017), and endocytic processes (Ilina et al., 2015). To investigate the putative mechanisms, uptake was assessed in the presence and absence of broad-spectrum transport (influx and efflux) and endocytosis inhibitors.

Methods

Materials

Pharmaceutical grade α-tocopherol polyethylene glycol succinate (TPGS) was purchased from BASF (Royal Tunbridge Wells, UK). Pharmaceutical grade polyvinyl alcohol (PVA grade 4–88, MW 57–77,000) was purchased from Merck KGaA (Darmstadt, Germany). Chloroform ($CHCl_3$) and dichloromethane (DCM) were purchased from Fisher Scientific (Loughborough, UK). Efavirenz was purchased from LGM Pharma (Chicago, USA) and donated by CIPLA (Mumbai, India). Endothelial Growth Basal Medium (EBM-2) media was purchased from Lonza (Slough, UK), and penicillin-streptomycin, chemically

defined lipid concentrate, and HEPES were purchased from Invitrogen (Paisley, UK). Fetal bovine serum gold was purchased from PAA, the Cell Culture Company (Cambridge, UK). The hCMEC/D3 cell line was a kind gift from Pierre-Olivier Couraud (INSERM, Paris, France). All other consumables were purchased from Sigma Aldrich (Dorset, UK).

Manufacture and physical characterisation of efavirenz solid drug nanoparticles

Preparation of emulsion-templated freeze-dried monoliths containing 70% efavirenz

Stock solutions of EFV (70 mg/mL in $CHCl_3$), PVA (22.5 mg/mL in water), and TPGS (22.5 mg/mL in water) were prepared. The three stock solutions were added to a sample tube in the ratio 100:90:45 (l μL) (EFV:PVA:TPGS) plus 265 μL water. The final solid mass ratio was therefore 70% EFV: 20% PVA: 10% TPGS (total solid mass 10 mg) in a 1:4 $CHCl_3$ to water mixture (total volume 0.5 mL). The sample was emulsified using a Covaris S2x acoustic homogenisation system for 30 sec with a duty cycle of 20, an intensity of 10, and 500 cycles/burst in frequency sweeping mode. Immediately after emulsification, the sample was cryogenically frozen and lyophilised using a Virtis benchtop K freeze-drier for 48 h. The white dry porous product was stored at ambient temperature prior to analysis.

Preparation of emulsion-templated freeze-dried monoliths containing 69% efavirenz labelled with 1% of the dye 1,1′-dioctadecyl-3,3,3′,3′-tetramethylindodicarbocyanine, 4-chlorobenzenesulfonate salt

Preparation followed the same procedure as described earlier; however, a sock solution of 70 mg/mL 1,1′-dioctadecyl-3,3,3′,3′-tetramethylindodicarbocyanine, 4-chlorobenzenesulfonate salt (DiD) was prepared in $CHCl_3$. The four stock solutions were added to a sample tube in the ratio 97:3: 90:45 (μL) (EFV:DiD:PVA:TPGS) plus 265 μL water. The final solid mass ratio was therefore 69% EFV: 1% DiD: 20% PVA: 10% TPGS (total solid mass 10 mg) in a 1:4 $CHCl_3$ to water mixture (total volume 0.5 mL). The blue dry porous product was stored at ambient temperature prior to analysis.

Preparation of emulsion-spray-dried powders containing 70% efavirenz

Stock solutions of EFV (280 mg/mL in DCM), PVA (50 mg/mL in water), and TPGS (50 mg/mL in water) were prepared. The three stock solutions were added to a sample tube in the ratio 16:25.6:12.8 (mL) (EFV:PVA: TPGS). The final solid mass ratio was therefore 70% EFV, 20% PVA: 10% TPGS (total solid mass 6.4 g) in a 1:2.4 DCM to water mixture (total volume 54.4 mL). The sample was emulsified using a Hielscher UP400S ultrasonic processor equipped with H7 Probe at 70% output (50 W) for 90 sec. Immediately after emulsification, the sample was spray dried on a benchtop spray dryer (BUCHI Mini-290) using an air-atomising nozzle and compressed air as the drying gas. Spray drying process conditions were 5 mL/min solution flow rate and 65°C outlet temperature. The white powder was collected and stored at room temperature before analysis.

Characterisation of aqueous efavirenz nanodispersions

Dynamic light scattering

Immediately prior to analysis, samples were dispersed by addition of water (1 mg/mL with respect to EFV content, therefore 7 mL for every 10 mg total solid mass) and vortex mixed to generate a uniform dispersion. Z-average diameter (D_z), zeta potential (ζ), polydispersity index (PDI), and number average diameter (D_n) were determined by dynamic light scattering (DLS) at a temperature of 25°C using a Malvern Zetasizer Nano ZS equipped with a 4 mW He–Ne, 633 nm laser, and using plastic disposable cuvettes. Malvern Zetasizer software version 7.03 was used for data analysis. ζ measurements were also carried out at 1 mg/mL, 25°C, and an initial pH of 6.5, using disposable capillary zeta cells. Dz , ζ, PDI, and D_n measurements were obtained as an average of three individual measurements and were obtained using the instrument's automatic optimisation settings.

Scanning electron microscopy

Scanning electron microscopy (SEM) images were recorded using a Hitachi S-4800 field emission instrument (SEM) at 3 kV. Dry samples were placed onto aluminium stub with carbon tabs. The samples were gold coated for 2 min at 15 mA using a sputter-coater (EMITECH K550X) prior to imaging.

Routine human cerebral microvessel endothelial cells/D3 culture

Human cerebral microvessel endothelial cells/D3 were cultured in EBM-2 media supplemented with fetal

bovine serum gold 5%, penicillin-streptomycin 1%, hydrocortisone 1.4 μM, ascorbic acid 5 μg/mL, chemically defined lipid concentrate 1/100, HEPES 10 mM, and bFGF 1 ng/mL. All culture flasks and plates were coated with rat collagen type 1 for 1 h prior to use. Cells were cultured at 37°C in 5% CO_2. Cells were passaged every 3–4 days when confluent.

3-(4,5-Dimethylthiazol-2-yl)-2,5-Diphenyltetrazolium bromide cytotoxicity assay

Cells were seeded on plates pre-coated with collagen at 100 μL of 1 × 10^5 cells/mL. The plates were then incubated for 24 h at 37°C in 5% CO_2 to allow cell adherence. Following incubation, the media was replaced with 100 μL of fresh media containing the drug at desired concentration (plus vehicle, 0.5% dimethyl sulfoxide). Positive and negative controls were represented by no cells (representing 100% cell death) and by cells cultured in the presence of a vehicle control (representing 100% cell viability), respectively. The cells were then incubated for 1 h. Following incubation with the drug, the media was removed and replaced by 20 μL of 3-(4,5-dimethylthiazol-2-yl)-2,5-diphenyltetrazolium bromide (MTT) reagent (5 mg/mL solution in Hanks balanced salt solution (HBSS)). The cells were incubated for 2 h in the MTT reagent. Following incubation, 100 μL of lysis buffer (50% N-N-dimethylformamide in water containing 20% sodium dodecyl sulphate, 2.5% glacial acetic acid and 2.5% HCl, pH 4.7) was added to each well. Cells were incubated overnight at 37°C in 5% CO_2 to allow complete cell lysis. Following incubation, the absorbance of each well was read using the TECAN GENios plate reader, with filters set to 560 nm.

Impact of inhibition of drug transporters on efavirenz cellular accumulation

Cells were seeded on pre-collagenated six-well plates at a density of 2 × 10^6/mL and allowed to adhere overnight. Media was aspirated and replaced with 1 mL fresh media containing 10 μM (0.014 μCi) of an aqueous solution of EFV or EFV SDNs (in the presence or absence of transporter inhibitors shown in Table 1) (Dickens et al., 2012). Cells were incubated at 37°C in 5% CO_2 in the presence of the drugs for 1 h. Following incubation, 100 μL of media was aspirated and added to scint vials with 4 mL goldstar scintillation fluid (extra cellular drug content). Cells were then washed with ice-cold HBSS ×3. Following washes, 1 mL of trypsin was added to the cells then incubated at 37°C in 5% CO_2 for 15 min. The trypsin was then aspirated and added to scint vials with 4 mL goldstar scintillation fluid (intracellular content). Cellular accumulation ratios (CAR) were calculated using the following formula (where DPM = disintegrations per minute):

$$CAR = \frac{(intracellular\ DPM / total\ cell\ colume)}{(extracellular\ DPM / extracellular\ volume)}$$

Cellular volumes were determined using the Scepter™ cell counter 2.0 (Merck Millipore, Billerica, USA). Cell volumes were taken from a mean of three replicates, hCMEC/D3 volume 2.27pl.

Table 1. Inhibitors of transporters or endocytosis that were employed in the study. Also shown are the mechanisms known to be inhibited with references.

Class	Inhibitor	Mechanism	Reference
Transporter inhibition	Amantadine	OCT1 and OCT2	(Dickens et al., 2012)
	Cyclosporine A	P-gp, BCRP	(Gupta et al., 2006, Dorababu et al., 2009)
	Naringin	OATP1A2	(Alfirevic et al., 2015)
	Corticosterone	OCT3	(Dickens et al., 2012)
Endocytosis inhibition	Dynasore	Clathrin-dependent endocytosis	(Kirchhausen et al., 2008, Barrias et al., 2010)
	Indomethacin	Calveoli-dependent endocytosis	(Yumoto et al., 2006)
	Cytochalasin B	Actin-dependent mechanisms (including macropinocytosis and phagocytosis)	(MacLean-Fletcher and Pollard, 1980; Kee et al., 2004)

Impact of endocytosis inhibition on efavirenz accumulation

Cells were seeded on pre-collagenated six-well plates at a density of 2×10^6/mL and allowed to adhere overnight. Media was aspirated and replaced with 1 mL fresh media containing dynasore (100 μM), indomethacin (100 μM), or cytochalasin B (5 μM) and incubated for 30 min at 37°C, 5% CO_2 (Table 1) (Kee et al., 2004; Sato et al., 2009). Following incubation, the media was aspirated and replaced with fresh media containing 10 μM of EFV aqueous solution formulation EFV or EFV SDNs. Cells were incubated at 37°C in 5% CO_2 in the presence of the drugs for 1 h. Following 1 h incubation, 1 mL of media was aspirated and added to 1.5 mL eppendorf tubes (extra cellular content). Cells were then washed with ice-cold HBSS ×3. Following washes, 1 mL of trypsin was added to the cells then incubated at 37°C in 5% CO_2 for 15 min. The trypsin was then aspirated and added to 1.5 mL eppendorf tubes (intracellular content). Samples were stored at −80°C until analysis via Liquid Chromatography Mass Spectrometry (LC-MS/MS).

$$CAR = \frac{(intracellular\ concentration)}{(extracellular\ concentration)}$$

Cellular volumes were determined using the Scepter™ cell counter 2.0 (Merck Millipore, Billerica, USA). Cell volumes were taken from a mean of three replicates, hCMEC/D3 volume 2.27pl.

Sample treatment and quantification of efavirenz via LC-MS/MS

Efavirenz was extracted by protein precipitation. A total of 20 μL of internal standard (lopinavir 1000 ng/mL) was added to 100 μL of sample (20% acetonitrile (ACN) was added to cell culture medium to aid EFV dissolution), standard or QC, which was then treated with 400 μL of ACN. Samples were then centrifuged at 4000 g for 10 min at 4°C. The supernatant fraction was transferred to a fresh glass vial and placed in a rotary vacuum centrifuge at 30°C to evaporate. Samples were then and reconstituted in 140 μL of H2O:ACN (60:40). A total of 100 μL of the sample was then transferred into 200 μL chromatography vials; 5 μL of each sample was injected for analysis.

Quantification was achieved via LC-MS/MS (TSQ Endura, Thermo Scientific) operating in negative mode (Curley et al., 2016). The following ions were monitored for quantification in selected reaction monitoring scan: EFV (m/z 315 > 242.1, 244.0 and 250.0) and internal standard, lopinavir (m/z 627 > 121.2, 178.1 and 198.1). A stock solution of 1 mg/mL EFV was prepared in methanol and stored at 4°C until use. A standard curve was prepared in EBM-2 cell culture medium by serial dilution from 500 to 1.9 ng/mL, and an additional blank solution was also used.

Chromatographic separation was achieved using a multistep gradient with a Hypersil gold C-18 column (Thermo scientific) using mobile phases A (100% H_2O, 5 mM NH_4HCO_2) and B (100% ACN, 5 mM NH_4HCO_2). Chromatography was conducted over 8.55 min at a flow rate of 300 μL/min. At the start of each run, mobile phase A was 90% until 0.1 min when mobile phase B was increased to 86% at 0.5 min. Mobile phase B was then gradually increased to 92% over 4.5 min. Mobile phase B was then increased to 97% at 5.1 min, which was held until 6 min. Mobile phase A was then increased to 90% and held till the termination of the run at 8 min. Inter-assay and intra-assay variance in accuracy and precision were <15%.

Assessing efavirenz solid drug nanoparticle uptake by flow cytometry

Cells were seeded on pre-collagenated six-well plates at a density of 2×10^6/mL and allowed to adhere overnight. Media was aspirated and replaced with 1 mL fresh media containing dynasore (100 μM), indomethacin (100 μM), or cytochalasin B (5 μM) and incubated for 30 min. Following incubation, media was aspirated and replaced with fresh media containing 10 μM of EFV SDNs containing 1% DiD or control (SDN DiD particles dissolved in 50% H_2O and 50% MeOH) (Liptrott et al., 2015). Cells were incubated at 37°C in 5% CO_2 in the presence of the drugs for 1 h. Following 1 h incubation, media was aspirated and cells were then washed with ice-cold HBSS ×3. Following washes, 1 mL of trypsin was added to the cells, then incubated at 37°C in 5% CO_2 for 5 min. The cells were then aspirated and transferred to 1.5 mL eppendorf tubes. Samples were then centrifuged at 2000 rpm for 5 min at 10°C. The trypsin was aspirated, and the cell pellet was resuspended in 500 μL of Macs buffer for analysis by flow cytometry using a MACSQuant analyser. Side scatter outcome was set to logarithmic and detected at a scattering angle of 90°. Flow rates were chosen such that less than 2000 events/s were recorded to prevent coincidence. For each measurement, a total number of 10,000 events were recorded (Liptrott et al., 2015). Data were analysed using MACSQuantify software.

Statistical analysis

All data were assessed for normality using the Shapiro–Wilk test. Statistical analysis was performed by unpaired *t*-test (for normally distributed data) or Mann–Whitney U test (for non-normally distributed data), and significance was defined as $P < 0.05$ (calculated in SPSS v21). All data are given as mean with standard deviation. IC_{50} values were calculated in Prism v6.0.

Results

Production and physical characterisation of efavirenz solid drug nanoparticles

The production of EFV SDNs was conducted using two emulsion-based techniques, ETFD and emulsion spray drying (ESD) (Fig. 1). Emulsion-templated freeze-drying utilises the rapid cryogenic freezing of an oil-in-water emulsion containing a volatile water-immiscible solvent dispersed phase containing dissolved hydrophobic compounds (Fig. 1A). The emulsion is stabilised by the presence of water-soluble polymers and surfactants within the continuous aqueous phase. Freeze-drying of the frozen emulsion leads to a porous monolithic structure, which readily disperses to yield stabilised nanoparticles of the hydrophobic compounds on addition of water (Zhang et al., 2008). The incorporation of two hydrophobic compounds within the dispersed organic phase leads to multi-component nanoparticles, and the inclusion of the fluorescer DiD to form EFV/DiD SDNs has been recently reported using ETFD (Giardiello et al., 2012; Liptrott et al., 2015). Dispersed dual-component EFV/DiD nanoparticles were analysed by DLS and shown to have an average hydrodynamic diameter (D_z) = 295 ± 25 nm with a PDI = 0.37. Zeta potential measurements ($\zeta = -18 \pm 0.5$ mV) were consistent with earlier reports.

Efavirenz SDNs were also formed using ESD, which rapidly dries the emulsion, containing EFV dissolved within the dispersed organic solvent phase, after atomisation into a stream of hot air (Fig. 1B). The spray dryer employed for this study utilised a two-fluid nozzle and generated spherical powder particles with sizes ranging from <1 to 10 μm, as judged by SEM imaging (Fig. 2).

The spray-dried powder particles showed a dimpled crust morphology (Fig. 2A and B) that is consistent with the external surface of the atomised droplets of emulsion drying quickly within the gas stream, followed by removal of residual volatile material (water and organic solvent) in subsequent stages (Fig. 1B). In contrast, SEM analysis of ETFD monoliths showed a convoluted open morphology (Fig. 2C and D) with little evidence of ice crystal growth or removal that may be seen in materials that have been freeze dried directly from aqueous solutions (Zhang et al., 2005). Dispersion of ESD powders into water resulted in nanodispersions that were also studied by DLS and found to have similar values to the ETFD SDNs containing 1 wt% DiD a D_z value of 250 ± 25 nm, PDI = 0.26, and $\zeta = -10 \pm 0.1$ mV.

The conformity of size and physical properties across the ETFD and ESD techniques suggested no inherent or meaningful difference (within error) between the two samples other than the presence of DiD. The use of the two techniques was required to allow correlation of the readily traceable EFV/DiD nanoparticles, produced by ETFD due to the prohibitive cost of DiD, with an ESD EFV nanoformulation that is progressing towards human clinical trial. Imaging of the SDN single and dual-component particles after dispersion is significantly hampered by the presence of water-soluble polymer and surfactant excipients as reported previously (Zhang et al., 2008).

Cytotoxicity of efavirenz solution, efavirenz solid drug nanoparticles, and inhibitors in human cerebral microvessel endothelial cells/D3 cells

Prior to accumulation studies, it was necessary to determine the concentrations of EFV in solution, EFV SDNs, and the various inhibitors that did not affect cell viability. To assess the cellular toxicity of the compounds used in accumulation studies, a concentration range of each drug was assessed using the MTT assay.

Table 1 summarises the IC_{50} data for all drugs and formulations used in the study. Efavirenz solution and EFV SDNs were assessed over the range of 0.19 μM to 100 μM EFV concentration. No statistically significant difference was observed in IC_{50} between the aqueous solution and the SDN ($P = 0.49$).

Transporter inhibitors were assessed over the final concentration range of 0.98 μM to 500 μM. The IC_{50} could not be generated for amantadine, cyclosporine A, naringin, or corticosterone as cytotoxicity was not observed under these conditions. Endocytosis inhibitors were assessed over the range of 0.39 to 200 μM. Similarly, the IC_{50} could not be generated for dynasore and indomethacin, as cytotoxicity was not observed under the experimental conditions.

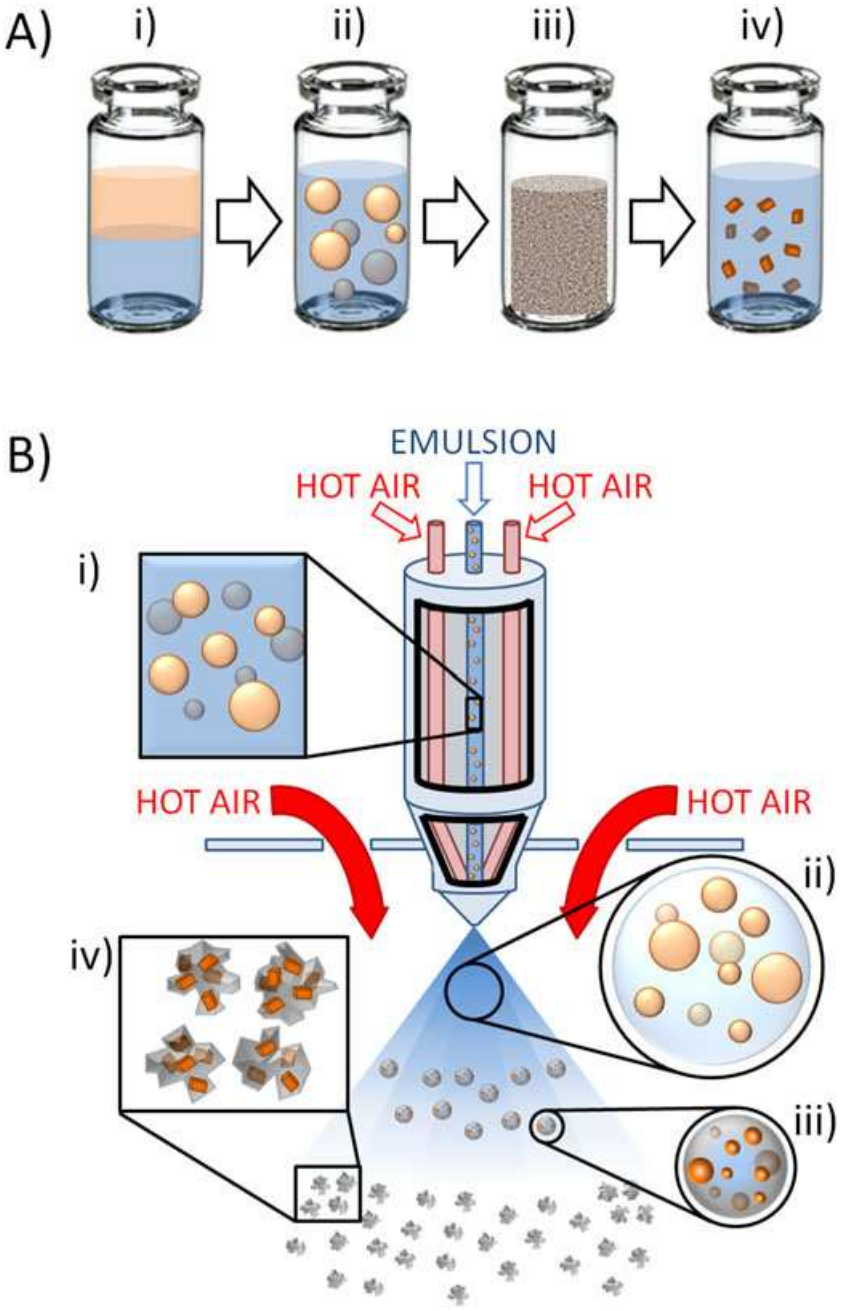

Figure 1. Schematic illustration of solid drug nanoparticle formation techniques. (A) Emulsion-templated freeze drying involves the following: (i) the dissolution of poorly soluble drug compound into a water-immiscible solvent and the dissolution of water-soluble excipients into water; (ii) emulsification; (iii) freezing and freeze-drying to yield a dry, porous monolith; and (iv) redispersion into water. (B) Emulsion spray drying involves the following: (i) the flow of the emulsion containing poorly soluble drug in the dispersed volatile organic phase and water-soluble excipients within the continuous phase through an atomiser, to form (ii) droplets of emulsion that rapidly dry in the hot air flow, initially forming (iii) a solidified crust with increased concentrations within the remaining liquid phase, and latterly, (iv) dry powder particles comprising solid drug nanoparticles within a dry excipient mixture.

Impact of drug transporter inhibition on efavirenz accumulation

Cellular accumulation studies were performed in the hCMEC/D3 cell line, and a panel of transporter inhibitors (Table 2) was employed to probe potential interactions with an EFV aqueous solution with transporters. Secondly, the accumulation of EFV SDNs in the presence of transporter inhibitors was probed to identify any differences in cellular accumulation due to nanoformulation (Fig. 3).

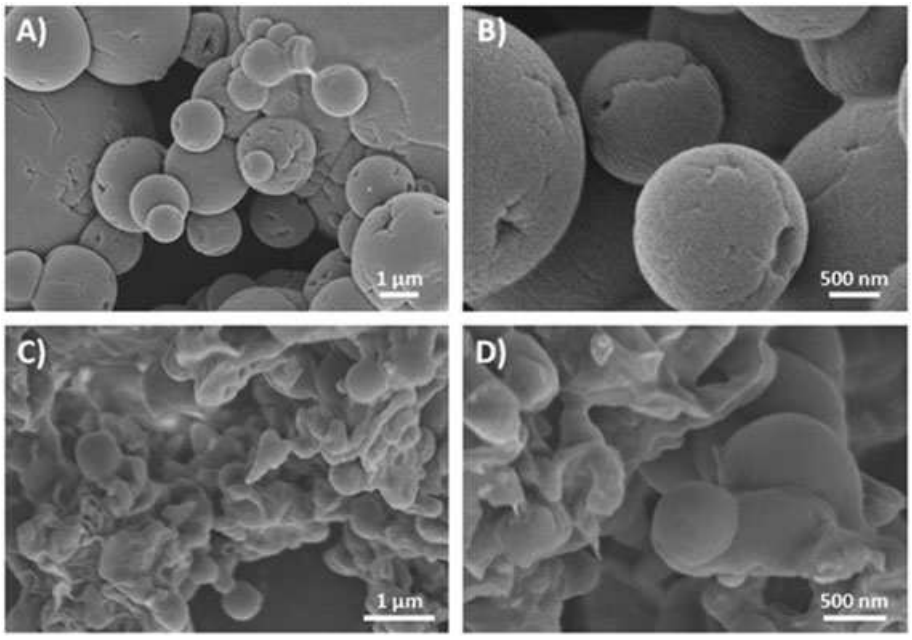

Figure 2. Scanning electron microscopy images of solid drug nanoparticle containing powders and monoliths: A&B) Emulsion spray dried powder particles, and C&D) internal morphology of emulsion template freeze dried monoliths. All images are structures prior to re-dispersion into water and release of solid drug nanoparticles.

Table 2. Cytotoxicity of all drugs and formulations used in the study in cerebral microvessel endothelial cells/D3 cells. IC_{50} values represent mean ± standard deviation.

Class	Drug	IC_{50} (µM, mean ± SD)
Aqueous solution (<1% DMSO)	Efavirenz	66.8 (21.32)
SDN aqueous dispersion	Efavirenz	57.6 (5.98)
Transport inhibitor	Amantadine	>500
	Cyclosporine A	>500
	Naringin	>500
	Corticosterone	>500
Endocytosis inhibitor	Dynasore	>200
	Indomethacin	>200
	Cytochalasin B	3.3 (2.88)

DMSO, dimethyl sulfoxide; SD, standard deviation; SDN, solid drug nanoparticle.

The screen of transporter inhibitors demonstrated no effect on the accumulation ratio of the EFV aqueous solution when in the presence of cyclosporine A (CAR = 70.3 ± 27.7, $P = 0.51$), naringin (CAR = 89.6 ± 8.1, $P = 0.18$), or corticosterone (CAR = 80.8 ± 12.5, $P = 0.96$). However, the accumulation ratio was reduced in the presence of amantadine (CAR 64.7 ± 6.0, $P = 0.03$).

The accumulation ratio of EFV after incubation with the SDN formulation was not affected by amantadine (CAR = 91. 9 ± 22.7, $P = 0.40$), cyclosporine A (CAR = 73.1 ± 17.2, $P = 0.40$), naringin (CAR = 89.1 ± 15.7, $P = 0.38$), or corticosterone (CAR = 77.2 ± 12.2, $P = 0.57$).

The effects of inhibitors of endocytosis on efavirenz accumulation

In addition to transport proteins, endocytosis is a potential mechanism for cellular uptake, especially for particulates. To probe the impact of endocytosis on the uptake of EFV aqueous solution and EFV SDNs, a

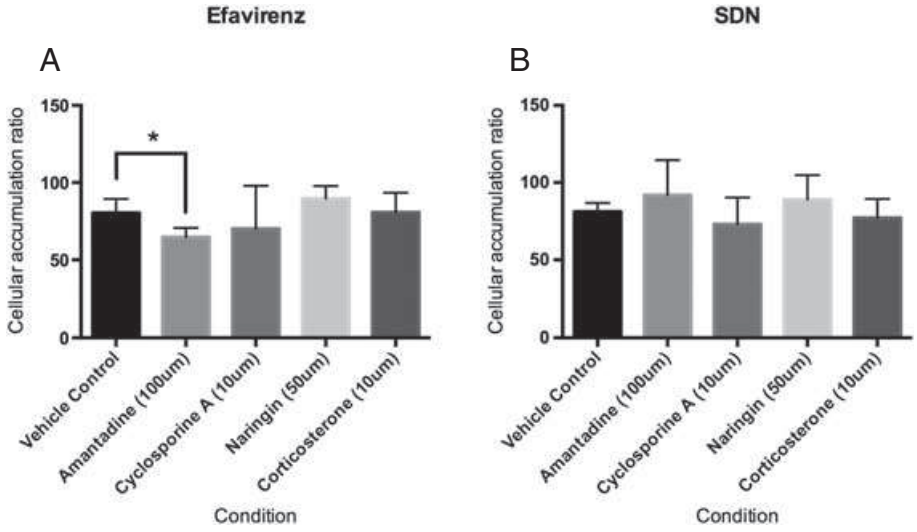

Figure 3. Shown are the cellular accumulation ratios generated for efavirenz (EFV) (A) and solid drug nanoparticle (SDN) efavirenz (B). Also shown are the cellular accumulation ratios in the presence of amantadine, cyclosporine A, naringin, and corticosterone. Data points indicate mean (±SD).

panel of endocytosis inhibitors was screened (Table 1) and the resulting data are presented in Figure 4.

The screen of endocytosis inhibitors demonstrated no effect on the accumulation ratio of either the aqueous solution (CAR = 92.7 ± 47.4) or SDNs (CAR = 118.7 ± 41.0) when in the presence of dynasore (aqueous CAR = 96.7 ± 13.1, P = 0.87, SDN CAR = 121.8 ± 18.0, P = 0.90), indomethacin (aqueous CAR = 137.6 ± 60.0, P = 0.29, SDN CAR = 119.4 ± 16.5, P = 0.98), or cytochalasin B (aqueous CAR = 96.5 ± 47.2, P = 0.91, SDN CAR = 141.4 ± 35.4, P = 0.43).

The effects of inhibitors of endocytosis on nanoparticle uptake using flow cytometry

The uptake of DiD-labelled EFV SDNs (4.02 ± 0.86 relative fluorescence units (RFU)) was significantly reduced (Fig. 5) by dynasore (0.91 ± 0.45 RFU, P = 0.001). Indomethacin had no effect on uptake of DiD-labelled EFV SDNs (3.44 ± 0.58 RFU, P = 0.307), whereas cytochalasin B significantly increased uptake (5.40 ± 0.70 RFU, P = 0.048; Fig. 6).

The uptake of dissolved DiD-labelled EFV-SDNs (8.75 ± 1.14 RFU) was significantly reduced by dynasore

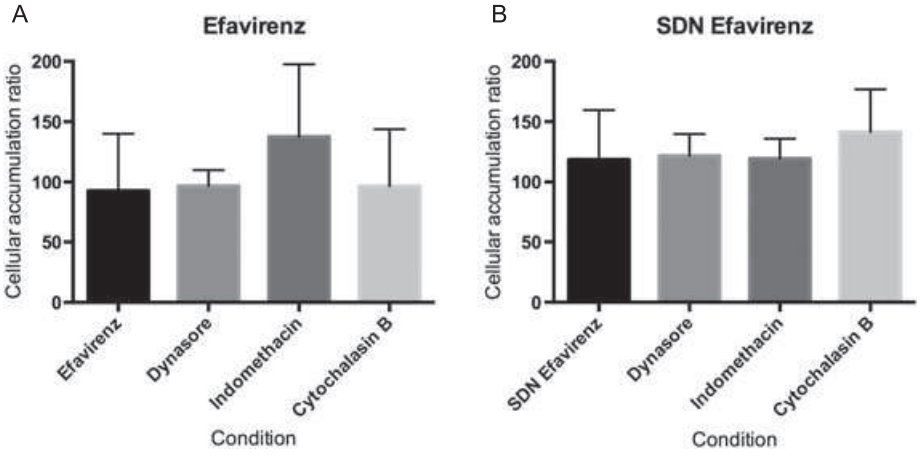

Figure 4. Shown are the cellular accumulation ratios generated for efavirenz (EFV) (A) and solid drug nanoparticle (SDN) EFV (B). Also shown are the cellular accumulation ratio in the presence of dynasore, indomethacin, and cytochalasin B. Data points indicate mean (±SD).

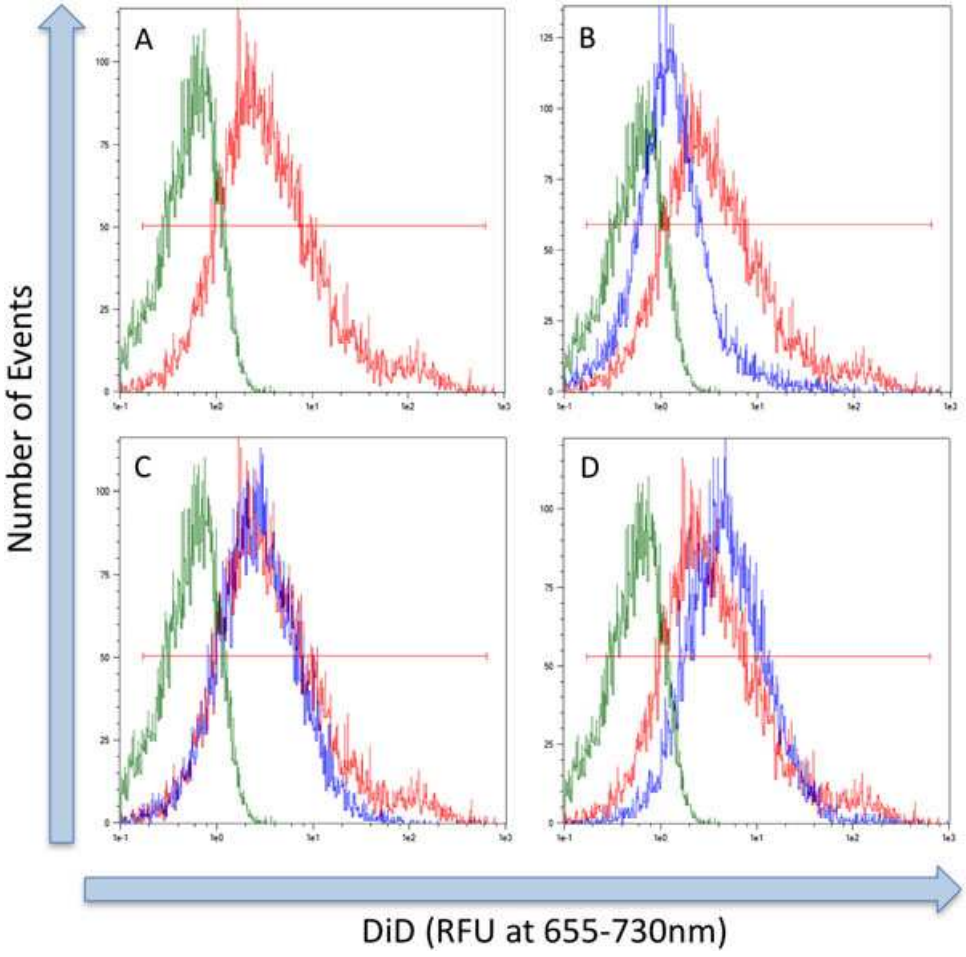

Figure 5. Scatter plot of the fluorescence detected at 655–730 nm. The green plot represents untreated cells (A–D). The red plot represents cells treated with DiD-labelled SDN (A–D). The blue plot represents the fluorescence in the presence of dynasore (B), indomethacin (C), and cytochalasin B (D).

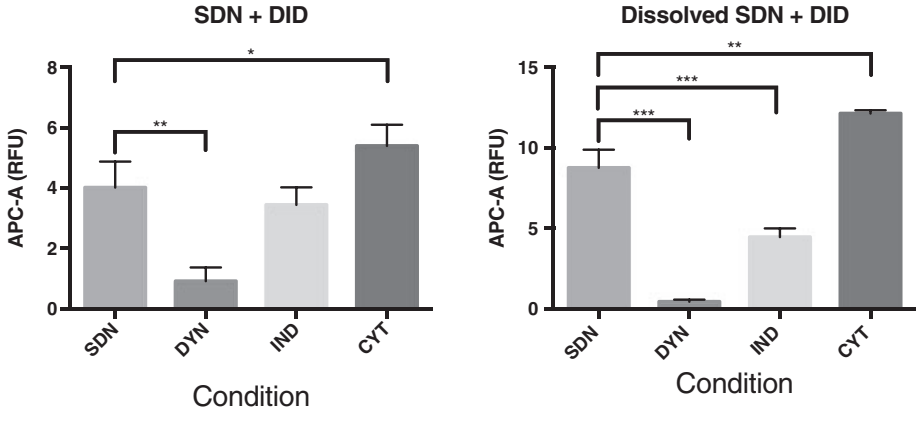

Figure 6. Shown is the fluorescence produced by cells treated with solid drug nanoparticle (SDN) 1,1′-dioctadecyl-3,3,3′,3′-tetramethylindodicarbocyanine, 4-chlorobenzenesulfonate salt (DiD) efavirenz (A) and dissolved SDN DiD efavirenz (B) in the presence of dynasore, indomethacin, and cytochalasin B. Data points indicate mean (±SD).

(0.43 ± 0.13 RFU, $P = <0.001$) and indomethacin (4.45 ± 0.54 RFU, $P = <0.001$). Cytochalasin B significantly increased the uptake of dissolved DiD-labelled EFV SDNs (12.12 ± 0.20 RFU, $P = <0.001$; Fig. 6).

Discussion

The data presented here demonstrated that cellular accumulation of aqueous EFV was reduced by amantadine (19.5% vs. control), but this was not the case when incubating with EFV SDNs. These data indicate that aqueous EFV may be a substrate for one of the OCT transporters and the SDN formulation may mitigate the influence of these transporters. Further transport studies are required to fully confirm these observations using multiple time points and a range of concentrations of substrate and inhibitor. The SDN formulation procedure generates particles with sizes of 322 ± 29 nm. Particles of this size are subjected to endocytosis, and nanoformulation has been used previously to reduce the impact of the transporter, BCRP (Canton and Battaglia, 2012; Wong et al., 2006). Further studies are required to fully elucidate the interactions of both the EFV aqueous solution and SDN formulations.

The data generated utilising the endocytosis inhibitors provided some contrasting data. When the drug accumulation ratio was examined, the endocytosis inhibitors had no effect on either the aqueous solution or the SDN formulation of EFV. Interestingly, uptake of the DiD-labelled SDNs was reduced by dynasore, indicating the role of dynamin-mediated uptake. However, the uptake of the dissolved DiD-labelled SDNs was reduced by both dynasore and indomethacin. This may indicate the incomplete dissolution of the SDN particles or that the dissolution process has altered the structure of the SDN particles, enabling uptake via calveoli-dependent endocytosis. The data also demonstrated higher uptake for the dissolved DiD SDN particles. This is not entirely unexpected, as DiD is a lypophilic dye and would be expected to readily pass through the lipid cell wall. This limitation could be resolved by the use of a cell impermeable dye, such as propidium iodide (fluorescence only observed when associated with intracellular nucleic acids). Propidium iodide has previously been incorporated into rhodamine B isothiocyanate-labelled silica nanoparticles to indicate cellular uptake (Neumeyer et al., 2011). These data indicate the importance of measuring both nanoparticle uptake and drug uptake. Although the drug concentrations may be equal in both preparations, the mechanism of cell entry and consequently intracellular fate may be significantly different.

The hCMEC/D3 cell line has been demonstrated to express many of the proteins found in the enterocytes of the BBB, making this cell line a suitable model for probing interactions at the BBB (Weksler et al., 2013). One of the limitations of the hCMEC/D3 cell line is the formation of tight junctions (Stanimirovic et al., 2015). The BBB is characterised by the presence of tight junctions, limiting paracellular transport. To fully replicate the presence of tight junctions, the hCMEC/D3 cell line requires technically demanding and prohibitively expensive culture conditions. It has been demonstrated to reproduce the tight junctions observed in vivo, but sheer stress induced by a pulsatile flow was required (Cucullo et al., 2008). Although accumulation experiments are useful for identifying potential mechanisms of uptake at the BBB, they do not demonstrate permeability across the BBB.

One of the limitations of investigating transporter interactions in cell lines is the lack of specificity in pharmacological transport inhibitors. Lack of specificity is also a consideration when examining inhibitors of endocytosis (Ivanov, 2008). In addition to other mechanisms of endocytosis, endocytosis inhibitors have also been shown to influence transport proteins, such as inhibition of ABCC1 by indomethacin (Leite et al., 2007). Cytochalasin B was shown to disrupt actin filaments and increase the intracellular accumulation of doxorubicin. Therefore, the conclusions that are drawn here are based on the known interactions of the inhibitors used but inhibition of other, as yet unknown processes cannot be ruled out with this strategy. Further studies utilising more specific methods (such as knock-down models, small interfering RNA, and oocyte uptake experiments) may be useful to complement in vivo studies and further elucidate the interactions relevant to distribution.

An additional limitation of the experimental design was that all experiments were conducted at 1 h. However, Liptrott et al. (2012) previously demonstrated that the CAR of EFV SDNs varied over 24 h in THP-1 cells, with the highest accumulation achieved within the first hour.

The presented data indicate that EFV SDNs may not traverse the BBB via the same mechanisms as dissolved EFV molecules. Amantadine significantly reduced EFV uptake, while there was no effect observed with the SDNs. In addition, dynasore reduced the uptake of DiD-labelled SDN particles indicating a role of dynamin-mediated endocytosis.

Funding Information

No funding information provided.

Conflict of Interest

AO and SR are co-inventors of patents relating to the application of nanotechnology to HIV drug delivery and are co-founders of a University of Liverpool start-up company, Tandem Nano Ltd. AO and SR have also received funding from Merck, Janssen, ViiV Healthcare, AstraZeneca, and Pfizer.

REFERENCES

Adkins, J. C., and S. Noble. **1998**. Efavirenz. Drugs *56*:1055–1064 discussion 1065-6.

Al-Ghananeem, A. M., Smith, M., Coronel, M. L., and H. Tran. **2013**. Advances in brain targeting and drug delivery of anti-HIV therapeutic agents. Expert Opin Drug Deliv *10*:973–985.

Alfirevic, A., Durocher, J., Elati, A., Leon, W., Dickens, D., Radisch, S., Box, H., Siccardi, M., Curley, P., Xinarianos, G., Ardeshana, A., Owen, A., Zhang, J. E., Pirmohamed, M., Alfirevic, Z., Weeks, A., and B. Winikoff. **2015**. Misoprostol-induced fever and genetic polymorphisms in drug transporters SLCO1B1 and ABCC4 in women of Latin American and European ancestry. Pharmacogenomics *16*:919–928.

Barrias, E. S., Reignault, L. C., De Souza, W., and T. M. Carvalho. **2010**. Dynasore, a dynamin inhibitor, inhibits Trypanosoma cruzi entry into peritoneal macrophages. PLoS One *5*:e7764.

Best, B. M., Koopmans, P. P., Letendre, S. L., Capparelli, E. V., Rossi, S. S., Clifford, D. B., Collier, A. C., Gelman, B. B., Mbeo, G., McCutchan, J. A., Simpson, D. M., Haubrich, R., Ellis, R., Grant, I., and C. Group. **2011**. Efavirenz concentrations in CSF exceed IC50 for wild-type HIV. J Antimicrob Chemother *66*:354–357.

Canton, I., and G. Battaglia. **2012**. Endocytosis at the nanoscale. Chem Soc Rev *41*:2718–2739.

Cucullo, L., Couraud, P. O., Weksler, B., Romero, I. A., Hossain, M., Rapp, E., and D. Janigro. **2008**. Immortalized human brain endothelial cells and flow-based vascular modeling: a marriage of convenience for rational neurovascular studies. J Cereb Blood Flow Metab *28*:312–328.

Curley, P., Siccardi, M., Moss, D. M., and A. Owen. **2016**. Development and validation of an LC-MS/MS assay for the quantification of efavirenz in different biological matrices. Bioanalysis *8*:2125–2134.

Dickens, D., Owen, A., Alfirevic, A., Giannoudis, A., Davies, A., Weksler, B., Romero, I. A., Couraud, P. O., and M. Pirmohamed. **2012**. Lamotrigine is a substrate for OCT1 in brain endothelial cells. Biochem Pharmacol *83*:805–814.

Dorababu, M., Nishimura, A., Prabha, T., Naruhashi, K., Sugioka, N., Takada, K., and N. Shibata. **2009**. Effect of cyclosporine on drug transport and pharmacokinetics of nifedipine. Biomed Pharmacother *63*:697–702.

Ene, L., Duiculescu, D., and S. Ruta. **2011**. How much do antiretroviral drugs penetrate into the central nervous system? J Med Life *4*:432.

Fellay, J., Marzolini, C., Meaden, E. R., Back, D. J., Buclin, T., Chave, J. P., Decosterd, L. A., Furrer, H., Opravil, M., Pantaleo, G., Retelska, D., Ruiz, L., Schinkel, A. H., Vernazza, P., Eap, C. B., Telenti, A., and H. I. V. C. S. Swiss. **2002**. Response to antiretroviral treatment in HIV-1-infected individuals with allelic variants of the multidrug resistance transporter 1: a pharmacogenetics study. Lancet *359*:30–36.

Giardiello, M., Mcdonald, T. O., Martin, P., Owen, A., and S. P. Rannard. **2012**. Facile synthesis of complex multi-component organic and organic-magnetic inorganic nanocomposite particles. J Mater Chem *22*:24744–24752.

Gupta, A., Dai, Y., Vethanayagam, R. R., Hebert, M. F., Thummel, K. E., Unadkat, J. D., Ross, D. D., and Q. Mao. **2006**. Cyclosporin A, tacrolimus and sirolimus are potent inhibitors of the human breast cancer resistance protein (ABCG2) and reverse resistance to mitoxantrone and topotecan. Cancer Chemother Pharmacol *58*:374–383.

Ilina, P., Partti, S., Niklander, J., Ruponen, M., Lou, Y. R., and M. Yliperttula. **2015**. Effect of differentiation on endocytic profiles of endothelial and epithelial cell culture models. Exp Cell Res *332*:89–101.

Ivanov, A. I. **2008**. Pharmacological inhibition of endocytic pathways: is it specific enough to be useful? Methods Mol Biol *440*:15–33.

Janneh, O., Chandler, B., Hartkoorn, R., Kwan, W. S., Jenkinson, C., Evans, S., Back, D. J., Owen, A., and S. H. Khoo. **2009**. Intracellular accumulation of efavirenz and nevirapine is independent of P-glycoprotein activity in cultured CD4 T cells and primary human lymphocytes. J Antimicrob Chemother *64*:1002–1007.

Kee, S. H., Cho, E. J., Song, J. W., Park, K. S., Baek, L. J., and K. J. Song. **2004**. Effects of endocytosis inhibitory drugs on rubella virus entry into VeroE6 cells. Microbiol Immunol *48*:823–829.

Kirchhausen, T., Macia, E., and H. E. Pelish. **2008**. Use of dynasore, the small molecule inhibitor of dynamin, in the regulation of endocytosis. Methods Enzymol *438*:77–93.

Leite, D. F., Echevarria-Lima, J., Calixto, J. B., and V. M. Rumjanek. **2007**. Multidrug resistance related protein (ABCC1) and its role on nitrite production by the murine macrophage cell line RAW 264.7. Biochem Pharmacol *73*:665–674.

Leschziner, G. D., Andrew, T., Pirmohamed, M., and M. R. Johnson. **2007**. ABCB1 genotype and PGP expression, function and therapeutic drug response: a critical review and recommendations for future research. Pharmacogenomics J *7*:154–179.

Leutscher, P. D., Stecher, C., Storgaard, M., and C. S. Larsen. **2013**. Discontinuation of efavirenz therapy in HIV patients due to neuropsychiatric adverse effects. Scand J Infect Dis *45*:645–651.

Liptrott, N. J., Giardiello, M., Hunter, J. W., Tatham, L., Tidbury, L. R., Siccardi, M., Rannard, S., and A. Owen. **2015**. Flow cytometric analysis of the physical and protein-binding characteristics of solid drug nanoparticle suspensions. Nanomedicine (Lond) *10*:1407–1421.

Liptrott, N. J., Martin, P., Giardiello, M., McDonald, T. O., Rannard, S. P., and A. Owen. **2012**. Solid Drug Nanoparticle Dispersions for Improved delivery of Efavirenz to Macrophages. British Pharmacological Society Winter Meeting, London, UK.

Maclean-Fletcher, S., and T. D. Pollard. **1980**. Mechanism of action of cytochalasin B on actin. Cell *20*:329–41.

McDonald, T. O., Giardiello, M., Martin, P., Siccardi, M., Liptrott, N. J., Smith, D., Roberts, P., Curley, P., Schipani, A., Khoo, S. H., Long, J., Foster, A. J., Rannard, S. P., and A. Owen. **2014**. Antiretroviral solid drug nanoparticles with enhanced oral bioavailability: production, characterization, and in vitro-in vivo correlation. Adv Healthc Mater *3*:400–411.

McDonald, T. O., Martin, P., Patterson, J. P., Smith, D., Giardiello, M., Marcello, M., See, V., O'reilly, R. K., Owen, A., and S. Rannard. **2012**. Multicomponent organic nanoparticles for fluorescence studies in biological systems. Adv Funct Mater *22*:2469–2478.

Mukherjee, S., Ghosh, R. N., and F. R. Maxfield. **1997**. Endocytosis. Physiol Rev *77*:759–803.

Neumeyer, A., Bukowski, M., Veith, M., Lehr, C. M., and N. Daum. **2011**. Propidium iodide labeling of nanoparticles

as a novel tool for the quantification of cellular binding and uptake. Nanomedicine *7*:410–419.
Peroni, R. N., Di Gennaro, S. S., Hocht, C., Chiappetta, D. A., Rubio, M. C., Sosnik, A., and G. F. Bramuglia. **2011**. Efavirenz is a substrate and in turn modulates the expression of the efflux transporter ABCG2/BCRP in the gastrointestinal tract of the rat. Biochem Pharmacol *82*:1227–1233.
Poller, B., Gutmann, H., Krahenbuhl, S., Weksler, B., Romero, I., Couraud, P. O., Tuffin, G., Drewe, J., and J. Huwyler. **2008**. The human brain endothelial cell line hCMEC/D3 as a human blood-brain barrier model for drug transport studies. J Neurochem *107*:1358–1368.
Raffi, F., Pozniak, A. L., and M. A. Wainberg. **2014**. Has the time come to abandon efavirenz for first-line antiretroviral therapy? J Antimicrob Chemother *69*:1742–1747.
Sanchez Martin, A., Cabrera Figueroa, S., Cruz Guerrero, R., Hurtado, L. P., Hurle, A. D., and A. Carracedo Alvarez. **2013**. Impact of pharmacogenetics on CNS side effects related to efavirenz. Pharmacogenomics *14*:1167–1178.
Sato, K., Nagai, J., Mitsui, N., Ryoko, Y., and M. Takano. **2009**. Effects of endocytosis inhibitors on internalization of human IgG by Caco-2 human intestinal epithelial cells. Life Sci *85*:800–807.
Sekhar, G. N., Georgian, A. R., Sanderson, L., Vizcay-Barrena, G., Brown, R. C., Muresan, P., Fleck, R. A., and S. A. Thomas. **2017**. Organic cation transporter 1 (OCT1) is involved in pentamidine transport at the human and mouse blood-brain barrier (BBB). PLoS One *12* e0173474.
Siccardi, M., Olagunju, A., Simiele, M., D'avolio, A., Calcagno, A., Di Perri, G., Bonora, S., and A. Owen. **2015**. Class-specific relative genetic contribution for key antiretroviral drugs. J Antimicrob Chemother *70*:3074–3079.
Stanimirovic, D. B., Bani-Yaghoub, M., Perkins, M., and A. S. Haqqani. **2015**. Blood-brain barrier models: in vitro to in vivo translation in preclinical development of CNS-targeting biotherapeutics. Expert Opin Drug Discovery *10*:141–155.
Weksler, B., Romero, I. A., and P. O. Couraud. **2013**. The hCMEC/D3 cell line as a model of the human blood brain barrier. Fluids Barriers CNS *10*:16.
Wong, H. L., Bendayan, R., Rauth, A. M., Xue, H. Y., Babakhanian, K., and X. Y. Wu. **2006**. A mechanistic study of enhanced doxorubicin uptake and retention in multidrug resistant breast cancer cells using a polymer-lipid hybrid nanoparticle system. J Pharmacol Exp Ther *317*:1372–1381.
Yilmaz, A., Price, R. W., and M. Gisslen. **2012**. Antiretroviral drug treatment of CNS HIV-1 infection. J Antimicrob Chemother *67*:299–311.
Yumoto, R., Nishikawa, H., Okamoto, M., Katayama, H., Nagai, J., and M. Takano. **2006**. Clathrin-mediated endocytosis of FITC-albumin in alveolar type II epithelial cell line RLE-6TN. Am J Physiol Lung Cell Mol Physiol *290*:L946–55.
Zhang, H., Hussain, I., Brust, M., Butler, M. F., Rannard, S. P., and A. I. Cooper. **2005**. Aligned two- and three-dimensional structures by directional freezing of polymers and nanoparticles. Nat Mater *4*:787–793.
Zhang, H., Wang, D., Butler, R., Campbell, N. L., Long, J., Tan, B., Duncalf, D. J., Foster, A. J., Hopkinson, A., Taylor, D., Angus, D., Cooper, A. I., and S. P. Rannard. **2008**. Formation and enhanced biocidal activity of water-dispersable organic nanoparticles. Nat Nanotechnol *3*:506–511.